microbial biotechnology

Open Access

One-pot synthesis of 6-aminohexanoic acid from cyclohexane using mixed-species cultures

Lisa Bretschneider, Martin Wegner, Katja Bühler, Bruno Bühler and Rohan Karande*

Department of Solar Materials, Helmholtz-Centre for Environmental Research –UFZ, Permoserstrasse 15, Leipzig, 04318, Germany.

Summary

6-Aminohexanoic acid (6AHA) is a vital polymer building block for Nylon 6 production and an FDA-approved orphan drug. However, its production from cyclohexane is associated with several challenges, including low conversion and yield, and severe environmental issues. We aimed at overcoming these challenges by developing a bioprocess for 6AHA synthesis. A mixed-species approach turned out to be most promising. Thereby, *Pseudomonas taiwanensis* VLB120 strains harbouring an upstream cascade converting cyclohexane to either ε-caprolactone (ε-CL) or 6-hydroxyhexanoic acid (6HA) were combined with *Escherichia coli* JM101 strains containing the corresponding downstream cascade for the further conversion to 6AHA. ε-CL was found to be a better 'shuttle molecule' than 6HA enabling higher 6AHA formation rates and yields. Mixed-species reaction performance with 4 g l^{-1} biomass, 10 mM cyclohexane, and an air-to-aqueous phase ratio of 23 combined with a repetitive oxygen feeding strategy led to complete substrate conversion with 86% 6AHA yield and an initial specific 6AHA formation rate of 7.7 ± 0.1 U g_{CDW}^{-1}. The same cascade enabled 49% 7-aminoheptanoic acid yield from cycloheptane. This combination of rationally engineered strains allowed direct 6AHA production from cyclohexane in one pot with high conversion and yield under environmentally benign conditions.

Introduction

Synthetic fibres, especially Nylon 6 and Nylon 66, account for 95% of the total polyamide production (Bellussi and Perego, 2000), with applications in the automotive, textile, electronics and packaging industries (Moody and Needles, 2004; BASF, 2020). The industrial synthesis of Nylon 6 from cyclohexane, with a scale of 4.2 million tons $year^{-1}$, involves multiple reaction steps and thus is highly resource-intensive (Ritz *et al*., 1986). With an industrial history of 75 years, it suffers from a low cyclohexane per pass conversion of 10–15%, multiple unit operations at high temperature and pressure variations, huge efforts necessary for intermediate product isolation, extensive waste generation, and formation of explosive intermediates (Fischer *et al*., 2010; Wittcoff *et al*., 2012). Thus, there is a growing demand to develop sustainable synthetic routes that allow high substrate conversion and product yield, with reduced waste generation and energy consumption (Bellussi and Perego, 2000). In this context, the one-pot (bio)synthesis of 6-aminohexanoic acid (6AHA as precursor of Nylon 6) from cyclohexane would offer a greener and more sustainable process route.

Sattler and coworkers demonstrated an *in vitro* approach combining 6 isolated enzymes to synthesize 6AHA from cyclohexanol (Sattler *et al*., 2014). Although balancing the enzyme ratio in the *in vitro* approach seems to be more straightforward than *in vivo*, finding the right enzymes with matching kinetics and catalytic efficiencies to synthesize 6AHA without accumulation of intermediate products turned out to be challenging (Sattler *et al*., 2014). However, the tedious purification of all enzymes, the provision of necessary cofactors and their respective regeneration systems, and enzyme instability under process conditions favour the use of whole-cell biocatalysts (Duetz *et al*., 2001; Walton and Stewart, 2004; Leak *et al*., 2009, Schrewe *et al*., 2013, Ladkau *et al*., 2014).

In past decades, advances in the metabolic engineering toolbox enabled the rational design and expression of complex biosynthetic pathways in a single host for the production of high-value chemicals (Ladkau *et al*., 2014). Although cascades involving more than 5 steps have been rationally engineered (Jeschek *et al*., 2017), several challenges including redox imbalance, excess metabolic burden, poor expression levels, and toxicity issues often resulted in low product yields (Muschiol *et al*., 2015; Rudroff, 2019). In this context, significant progress has been achieved by segregating complex pathways via the use of more than one engineered microbial strain and thus distributing the metabolic burden (Zhang and

Received 5 October, 2020; revised 14 December, 2020; accepted 14 December, 2020.
*For correspondence. E-mail rohan.karande@ufz.de; Tel. +49 341 235 48 22 71; Fax. +49 341 235 45 1286.
Microbial Biotechnology (2021) **14**(3), 1011–1025
doi:10.1111/1751-7915.13744

Wang, 2016; Jones and Wang, 2018). For example, the coupling of limonene synthesis and oxyfunctionalization in one *Escherichia coli* strain resulted in low perillyl acetate yield, which could be improved by distributing this complex reaction cascade among two recombinant *E. coli* strains (Willrodt *et al*., 2015). Recently, the Nylon 66 monomer adipic acid (AA) has been synthesized from cyclohexane employing a consortium of three *E. coli* strains achieving a conversion of 42% and > 99% AA yield (Wang *et al*., 2020).

In this study, we aimed at 6AHA production from cyclohexane in a one-pot approach with high conversion and yield. For this purpose, previously established *Pseudomonas taiwanensis* VLB120 strains containing cascades for the conversion of cyclohexane to ϵ-caprolactone (ϵ-CL) and/or 6-hydroxyhexanoic acid (6HA) (Schäfer *et al*., 2020) served as the basis. The respective biosynthetic pathways involve a cytochrome P450 monooxygenase (Cyp), a cyclohexanol dehydrogenase (CDH), a cyclohexanone monooxygenase (CHMO), and, facultatively, a lactonase (Lact). In this study, we set out to amend this cascade by the alcohol dehydrogenase AlkJ from *Pseudomonas putida* GPo1 (van Beilen *et al*., 2001) and the ω-transaminase CV2025 from *Chromobacterium violaceum* (Ladkau *et al*., 2016) to finally synthesize 6AHA from cyclohexane (Fig. 1A). In order to enable modularity and a high overall pathway flux, we distributed the pathway genes among two vectors and also considered a mixed-species approach, which requires efficient shuttling of appropriate pathway intermediates among the strains (Jones and Wang, 2018). Finally, the operation of resulting systems was investigated by varying biomass amounts, gas–liquid phase ratios, and cyclohexane amounts in the aqueous phase to maximize substrate conversion and 6AHA yield.

Results

In our previous study, *P. taiwanensis* VLB120 was established as a platform organism to produce the polycaprolactone monomers ε-CL and 6HA from cyclohexane (Schäfer *et al*., 2020). In the present work, we aimed to extend this biocatalytic reaction cascade for the production of 6AHA, the building block of Nylon 6 serving an even larger market (4.2 million tons per annum) than polycaprolactone (25,000 tons per annum) (Ritz *et al*., 1986; Weissermel and Arpe, 2008).

The alcohol dehydrogenase AlkJ and the transaminase CV2025 as suitable enzymes for the conversion of 6HA to 6AHA

In a previous study, an *in vitro* cascade for 6AHA synthesis from cyclohexanol has been demonstrated (Sattler *et al*., 2014). However, all tested alcohol dehydrogenases were unable to catalyse 6HA oxidation to 6-oxohexanoic acid. Therefore, a complex strategy of esterase-catalysed capping of the acid group of 6HA with methanol, followed by oxidation of the alcohol group, transamination, and ester hydrolysis was pursued and allowed 6AHA production with a 24% yield. We set out to address 6HA oxidation directly and hypothesized that the membrane-associated alcohol dehydrogenase AlkJ from *P. putida* GPo1 (van Beilen *et al*., 1994) bears high respective potential. AlkJ has been reported to convert aliphatic alcohols and ω-hydroxyfatty acid methyl esters to corresponding aldehydes with high specific activity, for example 79 U g_{CDW}^{-1} for 12-hydroxydodecanoic acid methyl ester oxidation in *E. coli* cells (Schrewe *et al*., 2014). Beside its promising substrate spectrum, the irreversible nature of AlkJ-catalysed alcohol oxidation constitutes a crucial advantage. Ubiquinone serves as electron acceptor for AlkJ, which thereby feeds electrons into the respiratory electron transport chain (Kirmair and Skerra, 2014). It remained to be elucidated, if AlkJ also accepts 6HA as substrate. For the conversion of the resulting product 6-oxohexanoic acid to 6AHA, the transaminase CV2025 (TA) originating from *C. violaceum* was selected. This enzyme is known to be active on long-chain aldehydes and amines carrying carboxylic acid groups (Kaulmann *et al*., 2007). It has successfully been applied together with AlkJ in a cascade hosted by *E. coli* JM101 to synthesize Nylon 12 monomers with fatty acid methyl esters as substrates (Ladkau *et al*., 2016). Here, we first tested AlkJ and TA cascade in *E. coli* JM101 (*E. coli*_6HA) for the conversion of 6HA to 6AHA.

Figure 2A demonstrates that the AlkJ-TA combination indeed catalyses the desired conversion of 6HA to 6AHA. A maximum specific whole-cell activity of 14.7 ± 1.2 U g_{CDW}^{-1} was achieved applying a 6HA concentration above 2.5 mM. Kinetic analyses involving the variation of the 6HA concentration revealed that as much as 1.5-2 mM 6HA was necessary to achieve half-maximal activity, an indication for a substrate uptake limitation (fitting with the Monod equation was not possible in this case). 6HA has a negative charge at the neutral pH applied, and its uptake may thus suffer from limited transfer over the cytoplasmic membrane. To investigate and circumvent such a 6HA uptake limitation, we constructed an *E. coli* strain (*E. coli*_CL), which, in addition to AlkJ and TA, encodes the highly active lactonase (Lact) derived from *Acidovorax* sp. CHX100 and is thus prone to accept uncharged ε-CL as a substrate. ε-CL can be expected to readily diffuse through outer membrane pores as well as the inner membrane. Indeed, *E. coli*_CL converted ε-CL into 6AHA with a high maximal activity of 39.4 ± 3.2 U g_{CDW}^{-1} (measured applying

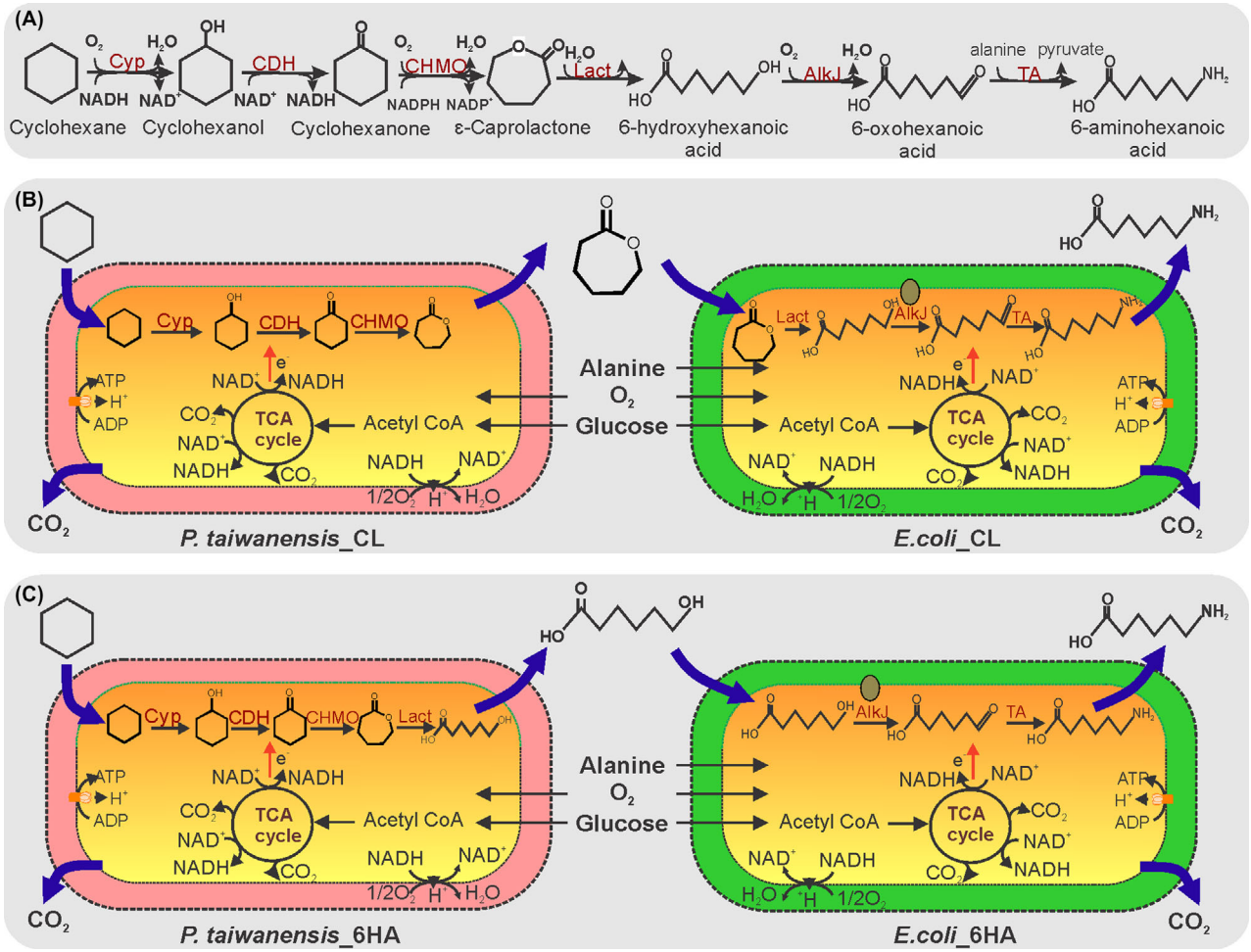

Fig. 1. Mixed-species strategies to produce 6-aminohexanoic acid (6AHA).A. Reaction scheme for the conversion of cyclohexane to 6AHA employing the enzymes Cytochrome P450 monooxygenase (Cyp), cyclohexanol dehydrogenase (CDH), cyclohexanone monooxygenase (CHMO), lactonase (Lact), alcohol dehydrogenase (AlkJ) and ω-transaminase (TA), (B) combination of *P. taiwanensis* VLB120 (pSEVA_CL_2) (*P. taiwanensis*_CL) and *E.coli* JM101 (pJ10Lact, pAlaDTA) (*E. coli*_CL) with ε-caprolactone (ε-CL) as shuttling compound, and (C) combination of *P. taiwanensis* VLB120 (pSEVA_6HA_2) (*P. taiwanensis*_6HA) and *E.coli* JM101 (pJ10, pAlaDTA) (*E. coli*_6HA) with 6-hydroxyhexanoic acid (6HA) as shuttling compound.

2.5 and 5 mM ε-CL) and featured an apparent ε-CL-related substrate uptake constant (K_S) of around 0.6 mM (fitted using the Monod equation) proving the substrate uptake limitation with 6HA as substrate (Fig. 2B). Next, the product formation pattern of *E. coli*_CL was analysed to get insight into enzyme activities and the rate-limiting step (Fig. 2C). An immediate accumulation of 6HA with *E. coli*_CL showed that the specific activity for the lactonase-catalysed first step (559 ± 6 U g_{CDW}^{-1}) was 14-fold higher than that for the downstream steps catalysed by AlkJ and TA. This demonstrated that the AlkJ-catalysed alcohol oxidation was the rate-limiting step to produce 6AHA from ε-CL. After overnight incubation, most of the intermediate product 6HA was converted to the main product 6AHA and a minor amount of adipic acid (AA) as a by-product. Overall, 6 mM of ε-CL were transformed to 86% 6AHA, 9% intermediate product 6HA, and 5% overoxidation product AA.

A mixed-species approach enables 6AHA production from cyclohexane

As a next step, we aimed to design a complete enzyme cascade catalysing the conversion of cyclohexane to 6AHA in one strain. From our previous work, *P. taiwanensis* VLB120 (pSEVA_CL_2) (*P. taiwanensis*_CL) and *P. taiwanensis* VLB120 (pSEVA_6HA_2) (*P. taiwanensis*_6HA) strains were available catalysing the conversion of cyclohexane to ε-CL and 6HA as main products with initial specific whole-cell activities of 43.4 ± 1.9 and 44.8 ± 0.2 U g_{CDW}^{-1} respectively (Schäfer *et al.*, 2020). These strains do not show any accumulation of pathway

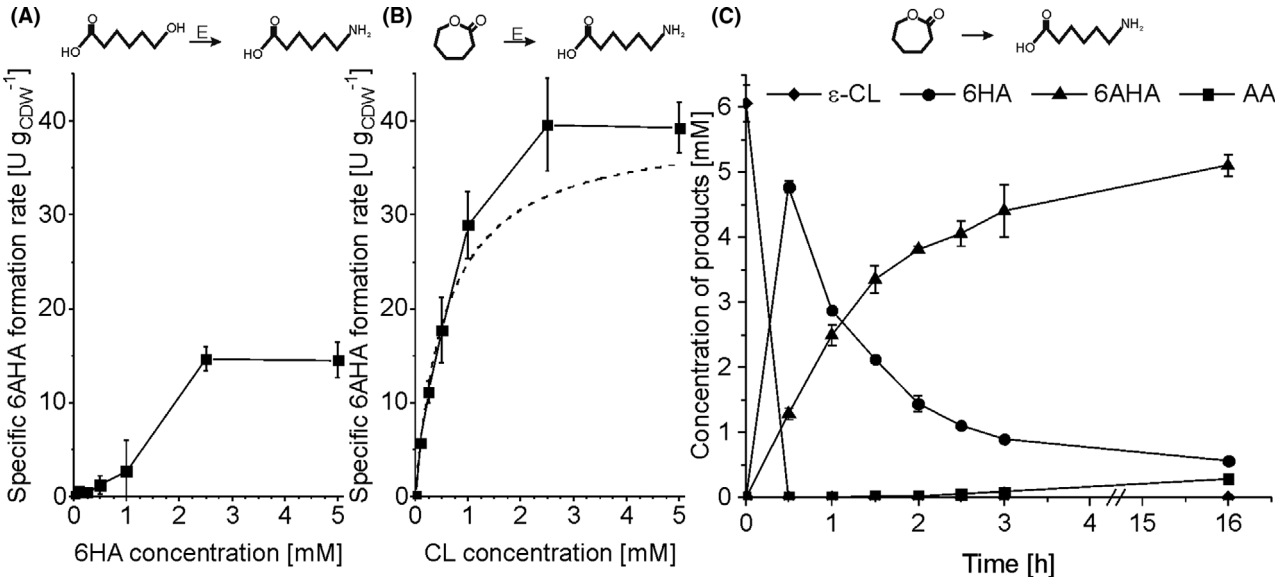

Fig. 2. Consecutive 6HA oxidation and transamination by recombinant *E. coli*. Panels A and B show specific 6AHA formation activities of *E. coli*_6HA (A) and *E. coli*_CL (B) at different initial substrate concentrations. Biotransformation assays were performed with a biomass concentration of 0.5 g_{CDW} l^{-1} in 10 ml liquid volume in 100 ml screw-capped and closed flasks for 30 min. The assay was started by ε-CL or 6HA addition. The dashed line in panel B depicts the curve according to Monod-type kinetics in order to determine the substrate concentration, at which the half-maximal rate is reached.C. Time-resolved product formation pattern for *E. coli*_CL. Biotransformation assays were performed with a biomass concentration of 1.5 g_{CDW} l^{-1} in 40 ml liquid volume in closed screw-capped 250 ml flasks and were started by adding 6 mM ε-CL. Means and error bars refer to two independent experiments. The average experimental errors over all measurements for specific 6AHA formation rates, ε-CL concentrations, 6HA concentrations, 6AHA concentrations and AA (adipic acid) concentrations are 32.7%, 4.6%, 2.0%, 5.3% and 3.9% respectively. E: *E. coli*-catalysed reactions.

intermediates at any time. However, the transfer of the *alkJ* containing *Pseudomonas*-compatible plasmids (Table S1, Entries 9, 11, 12) (Silva-Rocha *et al*., 2013) into *P. taiwanensis* VLB120 did not yield any 6HA oxidation activity, which disqualified *P. taiwanensis* as host for the expression plasmids studied. Possible reasons for the missing activity include improper folding and membrane association of AlkJ. On the other side, the transformation of *E. coli* JM101 with the plasmids pSEVA_CL_2 or pSEVA_6HA_2 did not give any colonies, possibly due to a high metabolic burden on the cells. Thus, a single strain approach employing *E. coli* or *Pseudomonas* as host strains appeared not to be feasible with the expression plasmids tested.

To circumvent these complications, we evaluated a mixed-species approach with recombinant *Pseudomonas* and *E. coli* cells for the catalysis of an upper and a lower part of the cascade respectively. For this purpose, the complex biocatalytic cascade for the production of 6AHA from cyclohexane was rationally segregated into two parts, an upstream cascade encoded by *P. taiwanensis*_CL or *P. taiwanensis*_6HA for the conversion of cyclohexane to ε-CL or 6HA and a downstream cascade catalysed by *E. coli*_CL or *E. coli*_6HA for the conversion of ε-CL or 6HA to the target product 6AHA respectively (Fig. 1B and C). In the former case, ε-CL served as the shuttling compound (Fig. 1B, 3 +3 approach), whereas this was the role of 6HA in the latter case (Fig. 1C, 4+2 approach). Both mixed-species approaches were investigated regarding cyclohexane conversion, specific rates, accumulation of intermediates, and 6AHA yield applying a strain ratio of 1:1, a total biomass concentration of 3 g_{CDW} l^{-1}, and 5 mM cyclohexane (referred to the aqueous phase volume). In both combinations, cyclohexanol, cyclohexanone and ε-CL concentrations remained below 50 μM. The specific activities within the first 3 h of reaction for total product formation and referring to the total cell concentration (both strains) were 8.1 ± 1.2 (Fig. 3A) and 9.0 ± 0.8 U g_{CDW}^{-1} (Fig. 3B) for the 3 + 3 and 4 + 2 cascades respectively. Consequently, the *Pseudomonas*-catalysed upper cascade was functional, with approximately 40% of its maximal activity. The specific activity for 6AHA formation was constant over the first 3 h with 4.3 ± 0.7 U g_{CDW}^{-1} for the 3 + 3 cascade, corresponding to 20% of its maximal activity (Fig. 2B), whereas, for the 4 + 2 cascade, it increased with time from below 1 U g_{CDW}^{-1}in the first hour to 4.3 ± 0.2 U g_{CDW}^{-1} in the third hour. The latter cascade with a high apparent K_S of *E. coli*_6HA for the shuttling compound 6HA (Fig. 2A) resulted in an overall slower 6AHA formation and 22% higher 6HA accumulation as

compared to the 3 + 3 cascade with ε-CL as major shuttling compound (Fig. 3B). Thereby, the 3 + 3 cascade reached a yield of 0.56 mol_{6AHA} $mol_{cyclohexane}$. These results favour the 3 + 3 cascade for 6AHA production from cyclohexane.

However, the accumulation of the intermediate product 6HA (27%), and the by-product AA (ca. 16%) due to inherent aldehyde dehydrogenase activities asked for further optimization to enhance the 6AHA yield. Aldehydes such as 6-oxohexanoic acid are generally very toxic to living cells (Feron *et al*., 1991) so that 'generic' dehydrogenases immediately convert them to their less toxic alcohol or acid derivatives (Wierckx *et al*., 2011). In this context, we aimed to enhance the rate for the downstream cascade by increasing the concentration of *E. coli* cells to 4 g_{CDW} l^{-1} while keeping the *P. taiwanensis* cell concentration constant at 1.5 g_{CDW} l^{-1}. This strategy, however, did not prevent 6HA and AA accumulation (Fig. S2). Whereas *P. taiwanensis*_CL showed similar activity as in the experiment shown in Fig. 3, *E. coli*_CL activity for 6AHA formation was low at only 10% of its maximal activity.

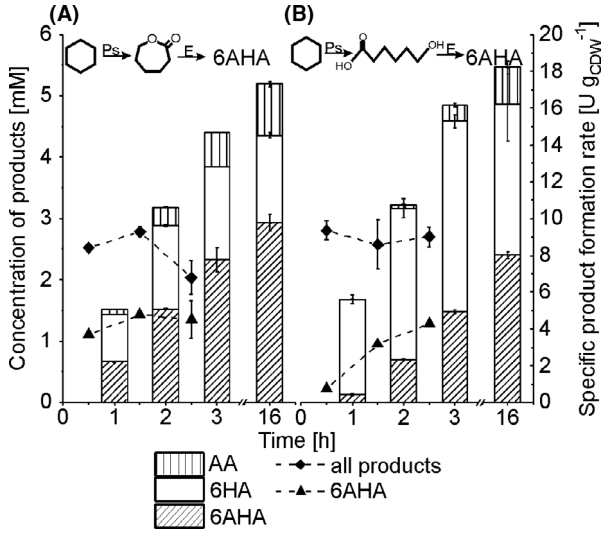

Fig. 3. Product formation from cyclohexane with the dual-species approach. The panels show the product concentrations accumulated after different reaction times (bars) and specific whole-cell activities over 3 h for 6AHA and overall product formation (curves). A 1:1 strain ratio was applied for the strain combinations *P. taiwanensis*_CL/*E. coli*_CL (A) and *P. taiwanensis*_6HA/*E. coli*_6HA (B). Biotransformations were performed with a total biomass concentration of 3.0 g_{CDW} l^{-1} in 10 ml liquid volume in closed screw-capped 100 ml flasks and were started by adding 5 mM cyclohexane (referred to the aqueous phase volume). Intermediate concentrations not depicted in the graphs remained below 50 μM. Means and error bars refer to two independent experiments. The average experimental errors over all measurements for specific product formation rates, 6HA concentrations, 6AHA concentrations and AA concentrations are 7.5%, 5.4%, 4.0% and 12.0% respectively. E: *E. coli*-based catalyst; Ps: *P. taiwanensis*-based catalyst.

Impact of mixed-species biomass concentration on catalytic performance and product formation pattern

Further critical factors possibly affecting cyclohexane conversion and 6AHA yield include the high volatility (vapour pressure: 0.12 atm), low water solubility (43 mg l^{-1} at 25°C), and toxicity of cyclohexane (National Center for Biotechnology Information, 2020). When added to the liquid phase in a closed flask, cyclohexane quickly evaporates and saturates the headspace, thus making the gas–liquid mass transfer a parameter, possibly influencing reaction performance. Furthermore, cyclohexane significantly affected *P. taiwanensis* VLB120 growth, with its growth rate being reduced by half at 0.4-0.5 mM cyclohexane in the aqueous phase (data not shown). Besides cyclohexane, oxygen availability and mass transfer also may influence the catalytic performance. Cyp and CHMO require oxygen as their direct co-substrate whereas AlkJ uses it as the terminal electron acceptor via the respiratory electron transport chain. A general impact of substrate (cyclohexane and O_2) availability was investigated by varying the biomass concentration utilizing a constant strain ratio of 1:1.

With 1 g_{CDW} l^{-1} biomass, specific activities within the first 2 h of reaction amounted to 18.9 ± 1.7 U g_{CDW}^{-1} for total product accumulation and 9.8 ± 1.6 U g_{CDW}^{-1} for 6AHA formation (Fig. 4 AB), which was 2-fold higher than the activity achieved with 3 g_{CDW} l^{-1} (Fig. 3A). Thereby, the upper cascade was operated at 87% of its maximal rate. After 2 h of reaction, these specific activities started to decrease significantly (Fig. 4A). Whereas the oxygen concentration still was around 15% (v/v) in the air phase and thus not limiting, the aqueous cyclohexane concentration stabilized and even slightly increased after 2 h of reaction (Fig. 4C). This cyclohexane level may have become rate-limiting or, more probably, inhibitory or toxic (over time – together with the products accumulated). After 16 h, a final cyclohexane conversion of 80% was achieved with a 6AHA yield of 47% (Fig. 4A and C). A volumetric rate of 0.59 mM_{6AHA} h^{-1} was accomplished over the first 2 h.

With 2 g_{CDW} l^{-1} biomass, cyclohexane was completely converted within the first 4 h of reaction. Within the first hour, specific rates amounted to 15.8 ± 1.3 U g_{CDW}^{-1} for total product formation and 7.4 ± 1.2 U g_{CDW}^{-1} for 6AHA formation and thus were similar to the initial rates achieved with 1 g_{CDW} l^{-1}. However, the 2-fold higher cell concentration increased the volumetric rate to 0.86 ± 0.12 mM_{6AHA} h^{-1} within the first 2 h. Within 4 h, the total product formation activity decreased from 16 U g_{CDW}^{-1} to 6 U g_{CDW}^{-1}, which correlated with the drop in the aqueous cyclohexane concentration (virtually depleted after 4 h) and thus cyclohexane limitation (Fig. 4B and C). A further increase of the biomass

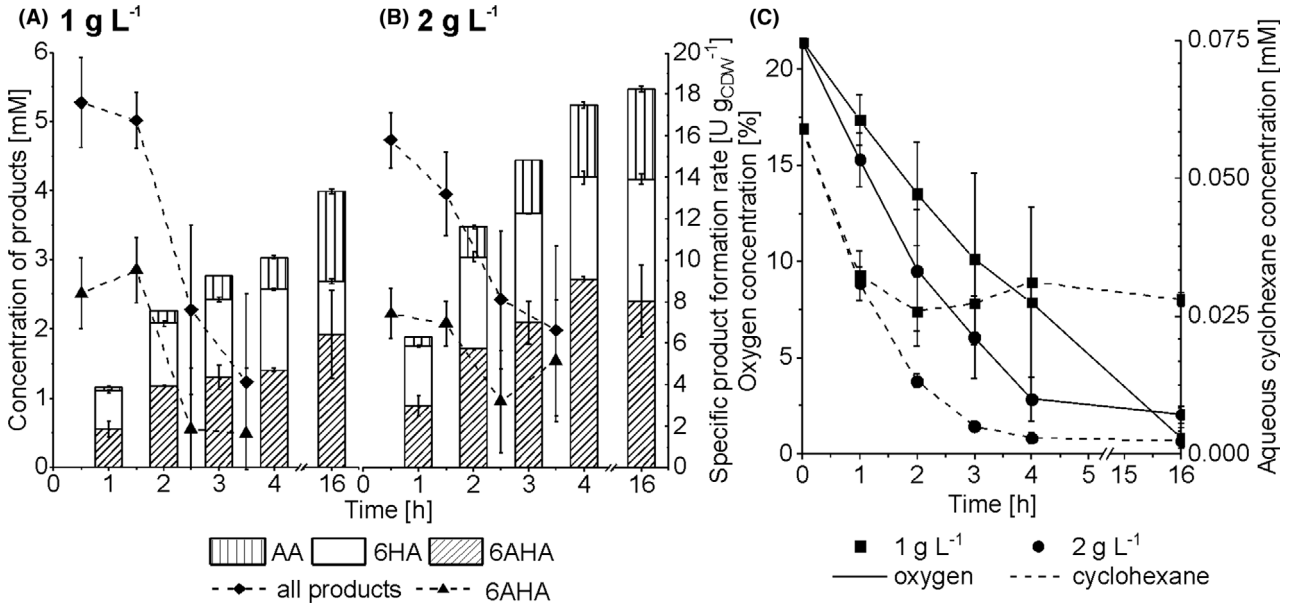

Fig. 4. Impact of mixed-species biomass concentration. Panels A and B show product concentrations accumulated after different reaction times (bars) and specific whole-cell activities over 4 h for 6AHA and overall product formation (curves). A 1:1 strain ratio was applied for the strain combination *P. taiwanensis*_CL/*E. coli*_CL with a total biomass concentration of 1.0 (panel A) or 2.0 g_{CDW} l^{-1} (panel B). Reactions were performed in 25 ml liquid volume in closed screw-capped 250 ml flasks and were started by adding 5 mM cyclohexane (referred to the aqueous phase volume). Intermediates not depicted in the graphs accumulated to less than 50 μM. Panel C shows the courses of oxygen concentrations in the gas phase (solid lines) and of aqueous cyclohexane concentrations (dashed lines). Means and error bars refer to two independent experiments. The average experimental errors over all measurements for specific product formation rates, 6HA concentrations, 6AHA concentrations, AA concentrations, oxygen concentrations and cyclohexane concentrations are 53.7%, 3.6%, 12.5%, 3.4%, 21.1% and 14.4% respectively. The high error for specific product formation rates results from the low product concentration changes.

concentration, as applied in the experiment shown in Fig. 3A, was thus not considered beneficial under the conditions applied. The oxygen content in the air phase had dropped below 2% after 4 h, which may have limited the catalytic activity of the downstream cascade (i.e. the respiration-dependent AlkJ activity) and thus further conversion of the accumulated 6HA (Fig. 4B and C). This resulted in a final conversion of 99% and a 6AHA yield of 44%. Overall, reaction conditions that overcome substrate limitation, oxygen limitation, and toxification were considered to be necessary to maximize the 6AHA yield.

Host-intrinsic dehydrogenase activity and oxygen availability severely influence the 6AHA yield

The interplay between cyclohexane and oxygen availability and mass transfer on 6AHA yield was further investigated by changing the air-to-liquid phase ratio from 11 to 23 and 5 by using 12.5 and 50 ml of liquid volume, respectively, in the closed Erlenmeyer flasks (Fig. 5). A biomass concentration of 3 g_{CDW} l^{-1} was applied to avoid a potential toxification by a prolonged presence of a high cyclohexane concentration. The reaction was initiated by adding 5 mM of cyclohexane to the aqueous phase, which, in a gas–liquid equilibrium, corresponded to aqueous phase concentrations of 28 and 128 μM with 12.5 and 50 ml liquid volume respectively (Fig. 5). At these concentrations, the upstream cascade in *P. taiwanensis* VLB 120 was expected to run at maximum reaction velocity or zero-order kinetics for 128 μM substrate and first-order kinetics for 28 μM substrate. By such variation of the initial reaction rate, we aimed to investigate its impact on cyclohexane conversion and 6AHA formation.

For 12.5 ml reaction volume, initial specific activities of total product formation (6.3 ± 1.0 U g_{CDW}^{-1}) and 6AHA formation (3.1 ± 0.4 U g_{CDW}^{-1}) were stable over 2 h (Fig. 5A). Due to cyclohexane limitation, the initial specific activities of total product formation were 25% lower than that in the same experiment with an air-to-liquid phase ratio of 11 (Fig. 3A). Again, host-intrinsic dehydrogenases, possibly in combination with AlkJ, affected high-level AA formation (53%), with a minimal amount of 6HA (6%) remaining at the end of the experiment. For 50 ml reaction volume, a high initial total specific activity of 19.0 ± 0.1 U g_{CDW}^{-1} in the first hour rapidly dropped to 1.2 ± 0.2 U g_{CDW}^{-1} in the second hour (Fig. 5B) correlating with a decrease in the gas-phase O_2 concentration from 21% to 2% within the first hour (Fig. 5C). The activity decrease can thus be attributed to O_2 limitation

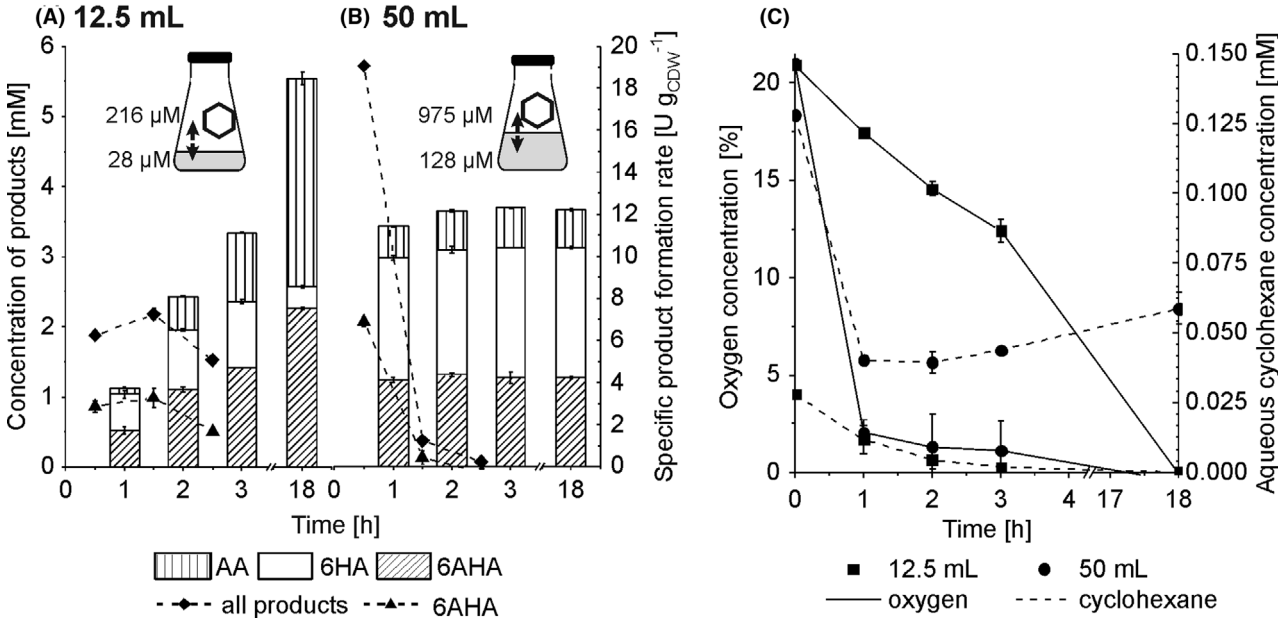

Fig. 5. Assessing the effect of O_2 and cyclohexane availability on by-product formation. Panels A and B show product concentrations accumulated after different reaction times (bars) and specific whole-cell activities over 3 h for 6AHA and overall product formation (curves). A 1:1 strain ratio was applied for the strain combination *P. taiwanensis*_CL/*E. coli*_CL with a total biomass concentration of 3.0 g l^{-1} in 12.5 (A) or 50 ml (B) liquid volume in 250 mll screw-capped and closed flasks. The biotransformation was started by adding 5 mM cyclohexane (referred to the aqueous phase volume). Intermediates that are not depicted in the graphs accumulated to less than 50 µM. The schemes of the reaction flasks show the calculated initial cyclohexane concentrations (µM) in the aqueous and gas phases in equilibrium. Panel C shows the courses of oxygen concentrations in the gas phase (solid lines) and of aqueous cyclohexane concentrations (dashed lines). Means and error bars refer to two independent experiments. The average experimental errors over all measurements for specific product formation rates, 6HA concentrations, 6AHA concentrations, AA concentrations, oxygen concentrations and cyclohexane concentrations are 39.2%, 3.4%, 3.2%, 2.3%, 14.2% and 22.9% respectively.

resulting in a final conversion of 73% and a 6AHA yield of 35% (Fig. 5B). From these results, we conclude that O_2 limitation and host-intrinsic dehydrogenase activity can severely affect the 6AHA yield.

Overcoming oxygen limitation and tuning cyclohexane hydroxylation rate to maximize 6AHA yield

Based on the results obtained, we aimed to select one-pot reaction conditions that allow complete cyclohexane conversion and maximum 6AHA yield. For this purpose, oxygen limitation was overcome by using a low liquid reaction volume of 12.5 ml in a 250 ml flask, an intermediary total biomass concentration of 2 g_{CDW} l^{-1}, and the addition of pure oxygen into the flask whenever the headspace oxygen concentration dropped below 10% (Fig. 6A and C). Thereby, the low reaction volume with 5 mM cyclohexane (with respect to the liquid volume) also was chosen to establish low cyclohexane concentrations in the aqueous phase and thus minimize potential toxification effects. The results obtained so far indicated that high cyclohexane levels especially hampered lower cascade performance (Figs 3-5), which is well conceivable as it couples to the respiratory chain considered to be especially sensitive to solvent toxicity due to its location in the cytoplasmic membrane (Buitelaar *et al*., 1990; Uribe *et al*., 1990; Vermuë *et al*., 1993; Revilla *et al*., 2007). At the chosen reaction conditions, cyclohexane was completely converted and, indeed, 6AHA was the main product with 82% yield (14% AA, 4% 6HA, Fig. 6A). The initial activity of 8.5 $\pm$ 0.5 U g_{CDW}^{-1} for total product formation indicates that the upper cascade was substrate limited, whereas the lower cascade could sustain a similar activity of 7.7 $\pm$ 0.1 U g_{CDW}^{-1}. These balanced rates of both cascade parts finally enabled the high 6AHA yield (Table 1). Additionally, we tested the conversion of 10 mM cyclohexane applying a total biomass concentration of 4 g_{CDW} l^{-1} in the same reaction set-up to evaluate the importance of synchronizing biomass and substrate concentration in the set-up chosen (Fig. S3). The initial specific activities for total product (9.7 $\pm$ 1.2 U g_{CDW}^{-1}) and 6AHA (7.7 $\pm$ 0.1 U g_{CDW}^{-1}) formation coincided with those obtained with 2 g_{CDW} l^{-1} and 5 mM cyclohexane (Table 1), resulting in 100% cyclohexane conversion and 86% 6AHA yield. Thereby, the higher substrate and biomass concentrations enabled a 2-fold increase in final 6AHA titre and volumetric productivity. Cyclohexane conversion and 6AHA yield obviously depend on substrate and biomass concentrations together with the avoidance of oxygen limitation.

Evidence for an extended substrate scope

The potential of the constructed catalysts and the mixed-species set-up was further evaluated for cycloheptane as a biotransformation substrate. By applying similar reaction conditions as for cyclohexane, complete conversion of 5 mM cycloheptane was obtained (Fig. 6B, Table 1). The initial activity for total product formation amounted to 8.5 $\pm$ 0.1 U g_{CDW}^{-1} and thus was comparable to the cyclohexane conversion activity obtained in the optimized set-up. After 18 h of biotransformation, 51% pimelic acid (PA), 48% 7-aminoheptanoic acid (7AHA) and 1% 7-hydroxyheptanoic acid (7HA) had accumulated (Fig. 6B). For the selected reaction conditions, the specific initial activity for 7AHA formation of 3.5 $\pm$ 0.1 U g_{CDW}^{-1} was lower than that for 6AHA formation (Table 1). Further optimization of reaction conditions is necessary for maximizing the 7AHA yield. However, the productivity and final 7AHA titre could again be doubled by doubling cycloheptane and biocatalyst concentrations (Table 1, Fig. S3B and C). Overall, the results obtained with cycloheptane as substrate indicate the broad applicability of the constructed strains and mixed-species set-up.

Discussion

In recent years, co-cultures have been applied to synthesize various compounds such as antibiotic building blocks (Zhang and Stephanopoulos, 2016), biofuels (Shin *et al.*, 2010), monoterpenoids (Willrodt *et al.*, 2015) or intermediates for polymer production (Zhang *et al.*, 2015; Wang *et al.*, 2020). In comparison with a single-species culture, the co-culture approaches are rationally designed to distribute the metabolic burden of long and complex biocatalytic pathways to different strains (Jones and Wang, 2018). However, the use of defined co-cultures requires the selection of compatible strains, easy access to shuttling compounds, and optimization of reaction conditions to achieve good biocatalytic performance.

Selection of biocatalysts to establish a mixed-species approach

The ability of AlkJ to oxidize ω-hydroxyacids and its tolerance towards the carboxylic acid moiety in 6HA were key findings in this work enabling the establishment of a more direct route for the transformation of cyclohexane to 6AHA compared previous studies (Sattler *et al.*,

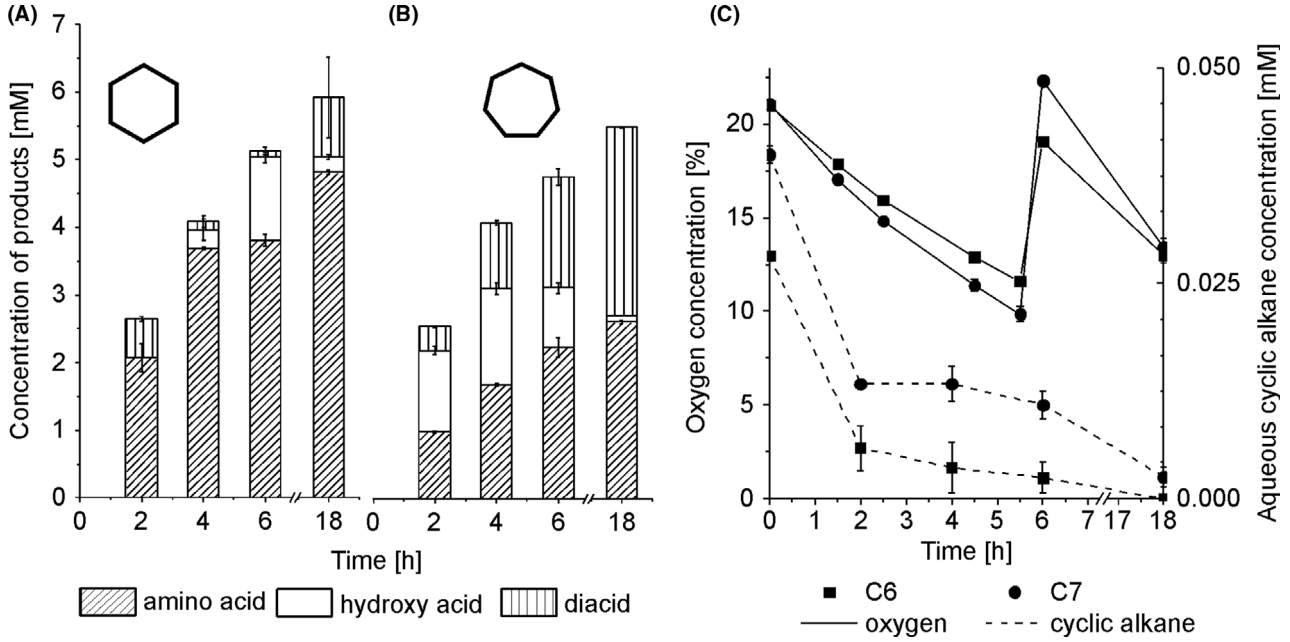

Fig. 6. Conversion of 5 mM cyclohexane (C6) or cycloheptane (C7) under optimized conditions. Panels A and B show product concentrations accumulated after different reaction times. A 1:1 strain ratio was applied for the strain combination *P. taiwanensis*_CL/*E. coli*_CL with a total biomass concentration of 2.0 g l^{-1} in 12.5 ml liquid volume in 250 ml screw-capped and closed flasks. Biotransformations were started by adding 5 mM of cyclohexane (A) or cycloheptane (B) (referred to the aqueous phase volume). Intermediates that are not depicted in the graphs accumulated to less than 50 μM. Panel C shows the courses of oxygen concentrations in the gas phase (solid lines) and of aqueous cyclohexane concentrations (dashed lines). Means and error bars refer to two independent experiments. The average experimental errors over all measurements for 6HA concentrations, 6AHA concentrations, AA concentrations, 7-hydroxyheptanoic acid concentrations, 7-aminoheptanoic acid concentrations, pimelic acid concentrations, oxygen concentrations, cyclohexane concentrations and cycloheptane concentrations are 25.6%, 3.4%, 52.0%, 5.0%, 2.1%, 3.8%, 1.5%, 65.6% and 15.7% respectively.

Table 1. Selected reaction parameters for the conversion of cyclohexane and cycloheptane

	Cyclohexane[a]		Cycloheptane[a]	
Initial substrate concentration[b]	5 mM	10 mM	5 mM	10 mM
Final 6-AHA titre [g l^{-1}]	0.63 ± 0.01	1.25 ± 0.10	0.34 ± 0.01	0.61 ± 0.04
6AHA productivity [mM h^{-1}]	0.92 ± 0.01 (4 h)	1.85 ± 0.01 (4 h)	0.42 ± 0.01 (4 h)	0.66 ± 0.03 (4 h)
	0.27 ± 0.01 (18 h)	0.53 ± 0.04 (18 h)	0.15 ± 0.01 (18 h)	0.26 ± 0.02 (18 h)
Conversion [%]	100	100	100	100
Selectivity for 6AHA [%]	81.6 ± 7.7	85.8 ± 2.7	47.7 ± 0.1	49.2 ± 1.2
Total initial activity[c] [U g_{CDW}^{-1}]	8.5 ± 0.5	9.7 ± 1.2	8.5 ± 0.1	7.0 ± 0.7
Initial 6AHA formation activity[c] [U g_{CDW}^{-1}]	7.7 ± 0.1	7.7 ± 0.1	3.5 ± 0.1	2.7 ± 0.1

a. A strain ratio of 1:1 was applied for the strain combination *P. taiwanensis*_CL/*E. coli*_CL with a total biomass concentration of 2.0 g l^{-1} (5 mM) or 4.0 g l^{-1} (10 mM) in 12.5 ml liquid volume in 250 ml screw-capped and closed flasks. Biotransformations were started by adding 5 or 10 mM of cyclohexane or cycloheptane (referred to the aqueous phase volume). Means and errors refer to two independent experiments. The average experimental errors over all measurements for final 6AHA titres, 6AHA productivity, conversions, selectivities for 6AHA and initial activities are 4.1%, 2.8%, 0, 3.8% and 4.5% respectively.
b. Referred to in aqueous phase.
c. For 4 h.

2014). Although AlkJ originated from the *Pseudomonas* genus (van Beilen *et al*., 2001) and can efficiently be synthesized in *E. coli* (Schrewe *et al*., 2014; Ladkau *et al*., 2016), recombinant expression of *alkJ* in *P. taiwanensis* VLB120 was not successful. On the other hand, employing *E. coli* for cyclohexane conversion was also not feasible, probably due to the high metabolic burden caused by the cytochrome P450 and Baeyer–Villiger monooxygenases. Even leaky expression of respective genes may have prevented successful transformation. For these enzymes, *E. coli* often does not constitute an optimal host organism (Biggs *et al*., 2016; Jones and Wang, 2018). Reasons include cofactor demand (e.g. heme), uncoupling involving the formation of reactive oxygen species, and drainage of cellular resources (redox equivalents, building blocks). More fine-tuned gene expression appears to be required to solve issues hampering upper and lower pathway expression in *E. coli* and *P. taiwanensis*, respectively, and finally may enable the establishment of a single strain catalysing 6AHA production from cyclohexane. However, the approach to distribute this complex biocatalytic pathway among *P. taiwanensis* and *E. coli* proved to be suitable for efficient 6AHA synthesis from cyclohexane and allowed to overcome the issues encountered in the single-species approaches. A similar approach was successful for the production of oxygenated taxanes (Zhou *et al*., 2015) and of ethanol from xylan (Shin *et al*., 2010). Besides alleviation of metabolic burden, mixed-species/strain approaches can be employed to circumvent inhibitory effects of pathway intermediates (Martínez *et al*., 2016), to meet cofactor and precursor requirements (Jones *et al*., 2016), or simply to establish physical compartmentalization for the prevention of sideproduct formation (Chen *et al*., 2017). Consequently, mixed-species cultures constitute a solid approach for the efficient operation of otherwise inefficient compex pathways/cascades by exploiting the capacities of two or more strains.

Selection of appropriate shuttle compounds in a mixed-species approach

The export and subsequent import of a shuttle compound that connects the pathway between the different species is a prerequisite for the efficient operation of a mixed-species set-up. The transport of organic acids, alcohols, simple sugars, amino acids, certain flavonoids and alkaloids can be realized by the selection of appropriate microbes (Zhang and Wang, 2016). The inner and outer membranes of Gram-negative bacteria, such as *E. coli* and *P. taiwanensis,* represent barriers for the diffusion of hydrophilic and large hydrophobic compounds, respectively (Leive, 1974). In this study, ε-CL and 6HA were investigated as possible shuttling compounds. Their small size (< 600 Da) allows them to pass the outer membrane by non-specific transmembrane pores (Denyer and Maillard, 2002; Nikaido, 2003). The inner membrane allows for passive diffusion of hydrophobic molecules but demands specific transport proteins for more hydrophilic compounds (Chen, 2007). 6HA is more polar than ε-CL and charged at the applied pH, leading to hampered transport of 6HA, as only its protonated form diffuses at a reasonable rate through the cytoplasmic membrane. This slower diffusion as compared to the ε-CL is reflected by the higher substrate concentration required for half-maximal activity (Fig. 2A and B). In certain cases, transporters such as AlkL, a hydrophobic outer membrane pore facilitating the passage of large hydrophobic molecules (Julsing *et al*., 2012), ShiA as a transporter for 3-dehydroshikimic acid (Zhang *et al*., 2015), or glycoside transporters (Shin *et al*., 2010) are required to enhance the transfer over the cellular

membrane. The membrane transfer rate of pathway intermediates thus can constitute a major limitation for the performance of a mixed-species approach. A careful selection of the intermediate or strain can enhance conversion.

Optimization of reaction conditions to maximize product yield

Co-cultivation of different species in growth mode is challenging due to possibly fluctuating community structures caused by differing induction times and growth rates (Jones and Wang, 2018). Avoidance of growth by the omission of a growth substrate other than the energy source, for example the N-source, constitutes a more straightforward approach. The different species can be grown separately according to their specific requirements (e.g. induction time, temperature) and then combined in defined ratios in a resting cell format (Willrodt *et al.*, 2015; Martínez *et al.*, 2016). In this study, a closed reaction system was required to avoid the loss of the volatile substrate cyclohexane. Figure 7 gives a schematic overview on substrate mass transfer and reaction rates. Gas–liquid mass transfer rates for cyclohexane (m_1) and O_2 (m_2) have a direct influence on r_1, the lumped rate of the three upper cascade reactions involving two oxygenases (Schäfer *et al.*, 2020), and r_3, the rate of AlkJ-catalysed 6HA oxidation, which is linked to the respiratory chain (Kirmair and Skerra, 2014). Furthermore, intrinsic dehydrogenases in both strains can convert 6-oxohexanoic acid into the by-product AA (r_5, r_6), thus minimizing 6AHA yield (Karande *et al.*, 2017; Schäfer *et al.*, 2020). Thereby, r_5 in *P. taiwanensis* also involves dehydrogenase-catalysed 6HA oxidation. The challenge was to minimize 6HA accumulation and AA formation.

Optimization of reaction conditions led us to utilize a gas–liquid phase ratio of 23 with biomass and cyclohexane concentrations of 2 g_{CDW} l^{-1} and 5 mM, respectively, as well as additional O_2 supply to avoid limitations of r_1 and r_3 (Fig. 6A and C). Under these conditions, m_1 governed overall cascade performance with the upstream cascade (r_1 = 1.02 mM h^{-1} (all products considered, first 4 h of reaction)) operated under first-order kinetics (Table 1, Fig. 6A and C). The effect of m_2 was minimized combining an appropriate biomass concentration with an O_2 feed. Due to the very high activity of the lactonase, the 6HA formation rate always was equal to the rate of ε-CL formation, $r_1 = r_2$. In set-ups only containg *E. coli*_CL (Fig. 2C) or *P. taiwanensis*_CL (Fig. S4), AA was formed at r_5 = 0.019 or r_6 = 0.041 mM h^{-1}, respectively (see Supporting Information, Section 3 for calculation details). However, within the first 4 h in the optimized mixed-species set-up (Fig. 6A), AA production rates ($r_5 + r_6$ = 0.03 mM h^{-1}) were well below the sum of

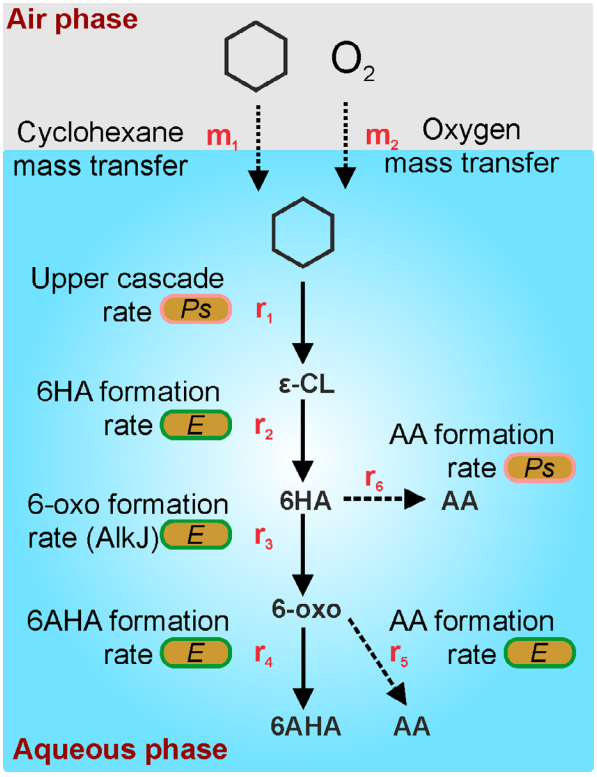

Fig. 7. Schematic representation of substrate mass transfer rates and cascade reaction rates in the mixed-species set-up designed in this study. The scheme refers to the consortium composed of *P. taiwanensis*_CL (*Ps*) and *E. coli*_CL (*E*). m_1, gas–liquid cyclohexane mass transfer; m_2, gas–liquid O_2 mass transfer; r_1, upper cascade reaction rate lumping the three reactions catalysed by *P. taiwanensis*_CL; r_2, rate of lactonase-catalysed ε-CL hydrolysis; r_3, rate of AlkJ-catalysed 6HA oxidation; r_4, rate of transaminase-catalysed 6AHA formation; r_5, rate of dehydrogenase-catalysed AA formation in *E. coli*_CL; r_6, rate of dehydrogenase-catalysed AA formation in *P. taiwanensis*_CL. If $m_1 < r_{1,max}$, the cascade performance is governed by cyclohexane mass transfer (substrate limitation). If $m_2 < 2r_{1,max} + r_{3,max}$, O_2 mass transfer becomes limiting. The high lactonase activity available led to $r_1 = r_2$. $r_2 > r_3$ leads to 6HA accumulation and possibly AA formation via r_6. $r_3 > r_4$ can lead to AA formation via r_5. $r_1 = r_2 = r_3 = r_4$ enables high 6AHA yield.

these rates. Thereby, r_6 may have been limited by 6HA availability/uptake. The volumetric 6AHA formation rate r_4 reached 0.92 mM h^{-1} (Table 1), which almost equalled r_3 = 0.92 – 0.95 mM h^{-1}, and thus enabled 100% cyclohexane conversion and 82% selectivity for 6AHA formation within 18 h. The step-wise assessment of crucial reaction parameters and their optimization allowed full cyclohexane conversion, which was not achieved previously (Wang *et al.*, 2020). In comparision with the biological process, a one-step chemical process using Mn/AlVPO resulted in 9.8% of cyclohexane conversion and 72.9% of selectivity to ϵ-caprolactam (You *et al.*, 2008).

Substrate limitation was selected in this study to minimize inhibition/toxification by cyclohexane and to avoid extensive 6HA accumulation. In the experiment shown in

Fig. 5A, the lower cascade did not reach its maximum rate and could not keep up with the upper cascade, although O_2 was not limiting and the necessary cyclohexane limitation was in place (Fig. 5C). This may be due to the different cyclohexane : biomass ratio applied (1.67 mmol g_{CDW}^{-1}) compared to the experiments shown in Fig. 6 (2.5 mmol g_{CDW}^{-1}, applied at two different concentration levels). This effect of the cyclohexane : biomass ratio and a possible interconnection with TA instability as indicated by AA accumulation (Fig. 5A) remain to be further investigated.

The low aqueous cyclohexane concentrations in the optimized set-up also can be considered beneficial regarding biocatalyst stability. With a logP of 3.44, cyclohexane is expected to cause membrane disintegration at a concentration above 0.6 mM (Sikkema *et al*., 1994) and, already at lower concentrations, can have effects on membrane fluidity, electron transduction, and, consequently, reactions connected to metabolism (Sikkema *et al*., 1994). Thus, cyclohexane can affect r_1 (via redox metabolism), r_3 (via electron transport chain), r_4 (via alanine uptake and regeneration) and r_5/r_6 (via redox metabolism). The establishement of an appropriate feeding regime will be crucial for future reaction engineering and scale up.

Further optimization may include strain ratio variation to equilibrate the rates of upstream and downstream cascades as demonstrated by Wang *et al*. (2020). The system presented here has been optimized regarding cyclohexane conversion and 6AHA yield and not specific activity. A higher *E. coli*_CL share can be considered promising to limit 6HA accumulation but has been tested without success (Fig. S2). However, O_2 depletion kinetics (Figs 4 and 5) indicate that cells were O_2-limited at the high cell concentration and low gas : liquid phase ratio applied in the respective experiment. Thus, strain ratio variation should be combined with a strategy to overcome O_2 limitation. Further, suppression of AA formation can be targeted via the knockout of 6-oxohexanoic acid oxidation catalysing dehydrogenases in both strains.

7AHA could be synthesized from cycloheptane by the same enzymes and mixed-species set-up, although the titre achieved was 2-fold lower than that obtained for 6AHA, going along with stronger overoxidation to PA. It is known that AlkJ also converts longer-chain substrates such as 12-oxododecanoic acid methyl ester with high activity (Schrewe *et al*., 2014). Thus, competition among TA and host dehydrogenases for 7-oxoheptanoic acid may be critical. In a previous study, it has been shown that the *C. violaceum* TA prefers small aliphatic and aromatic molecules (e.g. glyoxylate, butanal, benzaldehyde, phenylacetaldehyde) (Kaulmann *et al*., 2007). Hence, TA affinity for 7-oxoheptanoic acid constitutes a promising target to optimize the 7AHA yield, with enzyme engineering and screening of alternative TAs as possible approaches (Guo and Berglund, 2017).

Conclusion and future perspectives

This is the first study that demonstrates a one-pot biocatalytic synthesis of 6AHA and 7AHA from cycloalkanes with 100% conversion and high selectivities (86% and 49% respectively), which outcompete the one-pot chemical process with yields below 10% (You *et al*., 2008). Due to coexpression issues for the 8 genes required, the cascade was apportioned among *P. taiwanensis* and *E. coli*. As a shuttle compound, ϵ-CL turned out feasible as it readily diffuses through cell membranes enabling high 6AHA production rates. In shake flasks, the interplay between the cyclohexane and O_2 mass transfer and respective reaction rates was found to be critical for attaining a high 6AHA yield. Respective optimization of reaction conditions finally enabled the complete conversion of 10 mM cyclohexane with 86% 6AHA yield. For the technical scale, sophisticated feeding regimes and reaction engineering are prone to facilitate the balancing of oxygen and cyclohexane mass transfer and conversion rates. Suitable concepts include two-liquid phase systems (Kuhn *et al*., 2012) or a feed of cyclohexane-saturated air. Furthermore, the mixed-species phototrophic biofilm concept enabling continuous photosynthetic O_2 supply and operation at high cell densities (Hoschek *et al*., 2019) may be adapted for 6AHA production from cyclohexane. Besides the *in situ* oxygen supply, the utilization of light as the energy source and water as the electron source enabling redox cofactor regeneration constitutes another possible advantage of this approach, when cascade parts are implemented in phototrophic microbes.

Experimental procedures

Chemicals and media

Adipic acid was purchased from AppliChem (Darmstadt, Germany), 7-aminoheptanoic acid from chemPUR (Karlsruhe, Germany). 6-hydroxyhexanoic acid, 7-hydroxyheptanoic acid and cycloheptane were acquired from abcr (Karlsruhe, Germany). All other chemicals used in this study were obtained from Carl Roth GmbH + Co KG (Karlsruhe, Germany), Merck KGaA (Darmstadt, Germany) and Sigma Aldrich (Steinheim, Germany) in the highest purity available. Cells were grown in lysogeny broth medium (Sambrook and Russell, 2001) or M9* medium (Panke *et al*., 1999) with a pH of 7.2 supplemented with 0.5% (w/v) glucose as sole carbon source. Thiamine (10 mg l^{-1}), kanamycin (50 μg ml^{-1}) and chloramphenicol (35 μg ml^{-1}) were added when appropriate.

Strains, plasmids and molecular biology methods

The used strains and plasmids are listed in Table S1. *E. coli* JM101 and *P. taiwanensis* VLB120 were used for biotransformation studies and *E. coli* DH5α for cloning purposes. The preparation of electrocompetent *Pseudomonas* and *E. coli* cells was performed as described earlier (Sambrook and Russell, 2001; Choi and Schweizer, 2006), and the vectors were introduced by electroporation (2500 V; Eppendorf Eporator®, Hamburg, Germany). DNA manipulation methods and agarose gel electrophoresis were performed as described by Sambrook and Russell (2001). Enzymes (Phusion High-Fidelity Polymerase, T5 exonuclease, Taq ligase, restriction enzymes, Fast Alkaline Phosphatase) and buffers were purchased from Thermo Scientific Molecular Biology (St. Leon-Rot, Germany) or New England Biolabs (Frankfurt/Main, Germany) and oligonucleotides from Eurofins Genomics (Ebersberg, Germany). Plasmids were isolated using the peqGOLD Plasmid Miniprep Kit I from peqLab (Erlangen, Germany) and purified via NucleoSpin Gel and PCR Clean-up from Macherey–Nagel (Düren, Germany) according to supplier protocols. The Gibson Master Mix was prepared according to (Gibson *et al*., 2009). For detailed information, see Supporting Information (Section 1, Table S2).

Growth of bacterial cultures

Cultivations were carried out at 30°C and 200 rpm in a Multitron shaker (Infors, Bottmingen, Switzerland). Microorganisms were cultivated in an LB pre-culture for ~ 20 h, from which an M9* pre-culture (1% v/v) was inoculated and incubated for another 12-16 h. This pre-culture was used to inoculate an M9* main culture at a starting OD of 0.2. Heterologous gene expression was induced with 1 mM isopropyl β-d-1-thiogalactopyranoside (IPTG) for *P. taiwanensis* strains or 1 mM IPTG and 0.025% (v/v) (0.22 mM) dicyclopropyl ketone (DCPK) for *E. coli* strains when the cultures reached an OD of ~ 0.5. Incubation was continued for another 5 h until cells were harvested for the biotransformation experiments.

Biotransformation experiments

E. coli (pJ10, pAlaDTA) (*E. coli*_CL), *E. coli* (pJ10Lact, pAlaDTA) (*E. coli*_6HA), *P. taiwanensis* VLB120 (pSEVA_CL_2) (*P. taiwanensis*_CL), and *P. taiwanensis* VLB120 (pSEVA_6HA_2) (*P. taiwanensis*_6HA) were cultivated as described above. The cells were harvested by centrifugation (10 min, 3,214 g, room temperature) and resuspended in 100 mM potassium phosphate buffer (pH 7.4) supplemented with 1% (w/v) glucose and 50 mM L-alanine (reaction buffer) and thereby combined at different cell densities and strain ratios. The biotransformation assay was conducted in 100 or 250 ml screw-capped baffled Erlenmeyer flasks (total volumes of 123 ml and 300 ml respectively). The cell suspensions (volumes indicated in Table S3) were adapted for 10 min in a rotary incubator (30°C, 200 rpm). Biotransformation was initiated by adding pure substrate (cyclohexane, cycloheptane) to the concentration indicated in the text. The flask threads were wrapped with PTFE tape, and the lid contained a two-layered septum with Teflon facing the inner side of the flask and silicone facing outwards. A total of 1.5 ml samples were taken with a syringe at different time intervals. One ml sample was extracted with 0.5 ml ice-cold diethyl ether containing 0.2 mM n-decane as an internal standard. After 2 min extraction by vortexing and centrifugation, the organic phase was dried over water-free Na_2SO_4 before it was transferred to a GC vial for analysis. The rest of the samples was centrifuged (4°C, 10 min, 17,000 g), and the supernatant was stored for HPLC analysis. Gas-phase samples (100 μl) were taken from the flask using a gas-tight syringe (Hamilton, Reno, NV, USA). The activity is given in U g_{CDW}^{-1} (units per gram cell dry weight), where 1 U corresponds to 1 μmol product formed within 1 min reaction time. For specifications of biotransformation, set-ups refer to Table S3 in the Supporting Information. For analytical methods refer to Section 2 in the Supporting Information.

Acknowledgements

We acknowledge the use of the facilities of the Centre for Biocatalysis (MiKat) at the Helmholtz Centre for Environmental Research, which is supported by European Regional Development Funds (EFRE, Europe funds Saxony) and the Helmholtz Association. LB and RK were funded by the ERA-IB-Project PolyBugs ID:16006 and the Sächsisches Ministerium für Wissenschaft und Kunst (SMWK) Project ID: 100318259. The authors would like to thank Prof. Dr. Andreas Schmid for helpful discussions and Dr. Monika Möder and Steffi Schrader from the Department of Analytical Chemistry, Helmholtz Centre for Environmental Research – UFZ, for the help with HPLC-MS/MS.

Conflict of interest

None declared.

Funding information

We acknowledge the use of the facilities of the Centre for Biocatalysis (MiKat) at the Helmholtz Centre for

Environmental Research, which is supported by European Regional Development Funds (EFRE, Europe funds Saxony) and the Helmholtz Association. LB and RK were funded by the ERA-IB-Project PolyBugs ID: 16006 and the Sächsisches Ministerium für Wissenschaft und Kunst (SMWK) Project ID: 100318259.

References

BASF. (2020). *products & markets* [WWW document]. http://www2.BASF.us/businesses/plasticportal/products_and_markets.htm.

Bellussi, G., and Perego, C. (2000) Industrial catalytic aspects of the synthesis of monomers for nylon production. *Cattech* **4:** 4–16.

Biggs, B.W., Lim, C.G., Sagliani, K., Shankar, S., Stephanopoulos, G., De Mey, M., and Ajikumar, P.K. (2016) Overcoming heterologous protein interdependency to optimize P450-mediated Taxol precursor synthesis in *Escherichia coli*. *PNAS* **113:** 3209–3214.

Buitelaar, R., Vermue, M., Schlatmann, J., and Tramper, J. (1990) The influence of various organic solvents on the respiration of free and immobilized cells of *Tagetes minuta*. *Biotechnol Tech* **4:** 415–418.

Chen, R.R. (2007) Permeability issues in whole-cell bioprocesses and cellular membrane engineering. *Appl Microbiol Biotechnol* **74:** 730–738.

Chen, Z., Sun, X., Li, Y., Yan, Y., and Yuan, Q. (2017) Metabolic engineering of *Escherichia coli* for microbial synthesis of monolignols. *Metab Eng* **39:** 102–109.

Choi, K.-H., and Schweizer, H.P. (2006) mini-Tn7 insertion in bacteria with single *att*Tn7 sites: example *Pseudomonas aeruginosa*. *Nat Protoc* **1:** 153–161.

National Center for Biotechnology Information (2020). *Compound Summary: Cyclohexane* [WWW document]. URL https://pubchem.ncbi.nlm.nih.gov/compound/Cyclohexane.

Denyer, S.P., and Maillard, J.Y. (2002) Cellular impermeability and uptake of biocides and antibiotics in Gram-negative bacteria. *J Appl Microbiol* **92:** 35S–45S.

Duetz, W.A., Van Beilen, J.B., and Witholt, B. (2001) Using proteins in their natural environment: potential and limitations of microbial whole-cell hydroxylations in applied biocatalysis. *Curr Opin Biotechnol* **12:** 419–425.

Feron, V., Til, H., De Vrijer, F., Woutersen, R., Cassee, F., and Van Bladeren, P. (1991) Aldehydes: occurrence, carcinogenic potential, mechanism of action and risk assessment. *Mutat Res Genet Toxicol* **259:** 363–385.

Fischer, J., Lange, T., Boehling, R., Rehfinger, A., and Klemm, E. (2010) Uncatalyzed selective oxidation of liquid cyclohexane with air in a microcapillary reactor. *Chem Eng Sci* **65:** 4866–4872.

Gibson, D.G., Young, L., Chuang, R.-Y., Venter, J.C., Hutchison, C.A., and Smith, H.O. (2009) Enzymatic assembly of DNA molecules up to several hundred kilobases. *Nat Methods* **6:** 343–345.

Guo, F., and Berglund, P. (2017) Transaminase biocatalysis: optimization and application. *Green Chem* **19:** 333–360.

Hoschek, A., Heuschkel, I., Schmid, A., Bühler, B., Karande, R., and Bühler, K. (2019) Mixed-species biofilms for high-cell-density application of *Synechocystis* sp. PCC 6803 in capillary reactors for continuous cyclohexane oxidation to cyclohexanol. *Bioresour Technol* **282:** 171–178.

Jeschek, M., Gerngross, D., and Panke, S. (2017) Combinatorial pathway optimization for streamlined metabolic engineering. *Curr Opin Biotechnol* **47:** 142–151.

Jones, J.A., Vernacchio, V.R., Sinkoe, A.L., Collins, S.M., Ibrahim, M.H.A., Lachance, D.M., *et al*. (2016) Experimental and computational optimization of an *Escherichia coli* co-culture for the efficient production of flavonoids. *Metab Eng* **35:** 55–63.

Jones, J.A., and Wang, X. (2018) Use of bacterial co-cultures for the efficient production of chemicals. *Curr Opin Biotechnol* **53:** 33–38.

Julsing, M.K., Schrewe, M., Cornelissen, S., Hermann, I., Schmid, A., and Bühler, B. (2012) Outer membrane protein AlkL boosts biocatalytic oxyfunctionalization of hydrophobic substrates in *Escherichia coli*. *Appl Environ Microbiol* **78:** 5724–5733.

Karande, R., Salamanca, D., Schmid, A., and Buehler, K. (2017) Biocatalytic conversion of cycloalkanes to lactones using an in-vivo cascade in *Pseudomonas taiwanensis* VLB120. *Biotechnol Bioeng* **115:** 312–320.

Kaulmann, U., Smithies, K., Smith, M.E., Hailes, H.C., and Ward, J.M. (2007) Substrate spectrum of ω-transaminase from *Chromobacterium violaceum* DSM30191 and its potential for biocatalysis. *Enzyme Microb Technol* **41:** 628–637.

Kirmair, L., and Skerra, A. (2014) Biochemical analysis of recombinant AlkJ from *Pseudomonas putida* reveals a membrane-associated, flavin adenine dinucleotide-dependent dehydrogenase suitable for the biosynthetic production of aliphatic aldehydes. *Appl Environ Microbiol* **80:** 2468–2477.

Kuhn, D., Julsing, M.K., Heinzle, E., and Bühler, B. (2012) Systematic optimization of a biocatalytic two-liquid phase oxyfunctionalization process guided by ecological and economic assessment. *Green Chem* **14:** 645–653.

Ladkau, N., Assmann, M., Schrewe, M., Julsing, M. K., Schmid, A., and Bühler, B. (2016) Efficient production of the Nylon 12 monomer ω-aminododecanoic acid methyl ester from renewable dodecanoic acid methyl ester with engineered *Escherichia coli*. *Metab Eng* **36:** 1–9.

Ladkau, N., Schmid, A., and Bühler, B. (2014) The microbial cell—functional unit for energy dependent multistep biocatalysis. *Curr Opin Biotechnol* **30:** 178–189.

Leak, D.J., Sheldon, R.A., Woodley, J.M., and Adlercreutz, P. (2009) Biocatalysts for selective introduction of oxygen. *Biocatal Biotransformation* **27:** 1–26.

Leive, L. (1974) The barrier function of the Gram-negative envelope. *Ann N Y Acad Sci* **235:** 109–129.

Martínez, I., Mohamed, M.E.-S., Rozas, D., García, J.L., and Díaz, E. (2016) Engineering synthetic bacterial consortia for enhanced desulfurization and revalorization of oil sulfur compounds. *Metab Eng* **35:** 46–54.

Moody, V., and Needles, H.L. (2004) 3 - Major fibers and their properties. In *Tufted Carpet: Textile Fibers, Dyes, Finishes, and Processes*. Moody, V., and Needles, H.L. (eds). Norwich: William Andrew Publishing, pp. 35–59.

Muschiol, J., Peters, C., Oberleitner, N., Mihovilovic, M.D., Bornscheuer, U.T., and Rudroff, F. (2015) Cascade

catalysis–strategies and challenges *en route* to preparative synthetic biology. *ChemComm* **51:** 5798–5811.
Nikaido, H. (2003) Molecular basis of bacterial outer membrane permeability revisited. *Microbiol Mol Biol Rev* **67:** 593–656.
Panke, S., Meyer, A., Huber, C.M., Witholt, B., and Wubbolts, M.G. (1999) An alkane-responsive expression system for the production of fine chemicals. *Appl Environ Microbiol* **65:** 2324–2332.
Revilla, A.S., Pestana, C.R., Pardo-Andreu, G.L., Santos, A.C., Uyemura, S.A., Gonzales, M.E., and Curti, C. (2007) Potential toxicity of toluene and xylene evoked by mitochondrial uncoupling. *Toxicol In Vitro* **21:** 782–788.
Ritz, J., Fuchs, H., Kieczka, H., and Moran, W.C. (1986) Caprolactam. In *Ullmann's Encyclopedia of Industrial Chemistry*. Gerhartz, W. (ed). Weinheim: Wiley-VCH, pp. 31–50.
Rudroff, F. (2019) Whole-cell based synthetic enzyme cascades—light and shadow of a promising technology. *Curr Opin Chem Biol* **49:** 84–90.
Sambrook, J., and Russell, D. W. (2001) *Molecular Cloning: A Laboratory Manual*. Cold Spring Harbor, NY: Cold Spring Harbor Laboratory.
Sattler, J.H., Fuchs, M., Mutti, F.G., Grischek, B., Engel, P., Pfeffer, J., *et al*. (2014) Introducing an in situ capping strategy in systems biocatalysis to access 6-aminohexanoic acid. *Angew Chem Int Ed* **53:** 14153–14157.
Schäfer, L., Bühler, K., Karande, R., and Bühler, B. (2020) Rational engineering of a multi-step biocatalytic cascade for the conversion of cyclohexane to polycaprolactone monomers in *Pseudomonas taiwanensis*. *Biotechnol J* **15:** 2000091.
Schrewe, M., Julsing, M.K., Bühler, B., and Schmid, A. (2013) Whole-cell biocatalysis for selective and productive C-O functional group introduction and modification. *Chem Soc Rev* **42:** 6346–6377.
Schrewe, M., Julsing, M.K., Lange, K., Czarnotta, E., Schmid, A., and Bühler, B. (2014) Reaction and catalyst engineering to exploit kinetically controlled whole-cell multistep biocatalysis for terminal FAME oxyfunctionalization. *Biotechnol Bioeng* **111:** 1820–1830.
Shin, H.-D., McClendon, S., Vo, T., and Chen, R.R. (2010) *Escherichia coli* binary culture engineered for direct fermentation of hemicellulose to a biofuel. *Appl Environ Microbiol* **76:** 8150–8159.
Sikkema, J., de Bont, J.A., and Poolman, B. (1994) Interactions of cyclic hydrocarbons with biological membranes. *J Biol Chem* **269:** 8022–8028.
Silva-Rocha, R., Martínez-García, E., Calles, B., Chavarría, M., Arce-Rodríguez, A., de las Heras, A., *et al*. (2013) The Standard European Vector Architecture (SEVA): a coherent platform for the analysis and deployment of complex prokaryotic phenotypes. *Nucleic Acids Res* **41:** D666–D675.
Uribe, S., Rangel, P., Espínola, G., and Aguirre, G. (1990) Effects of cyclohexane, an industrial solvent, on the yeast *Saccharomyces cerevisiae* and on isolated yeast mitochondria. *Appl Environ Microbiol* **56:** 2114–2119.
van Beilen, J.B., Kingma, J., and Witholt, B. (1994) Substrate specificity of the alkane hydroxylase system of *Pseudomonas oleovorans* GPo1. *Enzyme Microb Technol* **16:** 904–911.
van Beilen, J.B., Panke, S., Lucchini, S., Franchini, A.G., Röthlisberger, M., and Witholt, B. (2001) Analysis of *Pseudomonas putida* alkane-degradation gene clusters and flanking insertion sequences: evolution and regulation of the *alk* genes. *Microbiology* **147:** 1621–1630.
Vermuë, M., Sikkema, J., Verheul, A., Bakker, R., and Tramper, J. (1993) Toxicity of homologous series of organic solvents for the gram-positive bacteria *Arthrobacter* and *Nocardia* Sp. and the gram-negative bacteria *Acinetobacter* and *Pseudomonas* Sp. *Biotechnol Bioeng* **42:** 747–758.
Walton, A.Z., and Stewart, J.D. (2004) Understanding and improving NADPH-dependent reactions by nongrowing *Escherichia coli* cells. *Biotechnol Prog* **20:** 403–411.
Wang, F., Zhao, J., Li, Q., Yang, J., Li, R., Min, J., *et al*. (2020) One-pot biocatalytic route from cycloalkanes to α, ω-dicarboxylic acids by designed *Escherichia coli* consortia. *Nat Commun* **11:** 1–10.
Weissermel, K., and Arpe, H.-J. (2008) *Industrial Organic Chemistry*. Hoboken, NJ: John Wiley & Sons, p. 511.
Wierckx, N., Koopman, F., Ruijssenaars, H.J., and de Winde, J.H. (2011) Microbial degradation of furanic compounds: biochemistry, genetics, and impact. *Appl Microbiol Biotechnol* **92:** 1095–1105.
Willrodt, C., Hoschek, A., Bühler, B., Schmid, A., and Julsing, M.K. (2015) Coupling limonene formation and oxyfunctionalization by mixed-culture resting cell fermentation. *Biotechnol Bioeng* **112:** 1738–1750.
Wittcoff, H.A., Reuben, B.G., and Plotkin, J.S. (2012) *Industrial Organic Chemicals*. Hoboken, NJ: John Wiley & Sons.
You, K., Mao, L., Chen, L., Yin, D., Liu, P., and Luo, H.A. (2008) One-step synthesis of ε-caprolactam from cyclohexane and nitrosyl sulfuric acid catalyzed by VPO supported transition metal composites. *Catal Commun* **9:** 2136–2139.
Zhang, H., Li, Z., Pereira, B., and Stephanopoulos, G. (2015) Engineering *E. coli–E. coli* cocultures for production of muconic acid from glycerol. *Microb Cell Fact* **14:** 134.
Zhang, H., and Stephanopoulos, G. (2016) Co-culture engineering for microbial biosynthesis of 3-amino-benzoic acid in *Escherichia coli*. *Biotechnol J* **11:** 981–987.
Zhang, H., and Wang, X. (2016) Modular co-culture engineering, a new approach for metabolic engineering. *Metab Eng* **37:** 114–121.
Zhou, K., Qiao, K., Edgar, S., and Stephanopoulos, G. (2015) Distributing a metabolic pathway among a microbial consortium enhances production of natural products. *Nat Biotechnol* **33:** 377.

Supporting information

Additional supporting information may be found online in the Supporting Information section at the end of the article.

Fig. S1. Oxygen measurement by GC. The panels show the GC chromatograms for a sample of 100% nitrogen (A) and air (B).

Fig. S2. Application of *P. taiwanensis* and *E. coli* strains at a lower strain ratio. The panels show the product concentrations accumulated after different reaction times (bars) and specific whole-cell activities over 3 h for 6AHA and overall product formation (curves). For the strain combinations *P. taiwanensis*_CL/*E. coli*_CL (**A**) and *P. taiwanensis*_6HA/*E. coli*_6HA (**B**), biotransformations were performed with biomass concentrations of 1.5 and 4 gCDW l^{-1} *P. taiwanensis* and *E. coli* strains, respectively, in 25 ml liquid volume in closed screw-capped 250 ml flasks and were started by adding 5 mM cyclohexane (referred to the aqueous phase volume). Intermediate concentrations not depicted in the graphs remained below 50 μM. Means and error bars refer to two independent experiments. The average experimental errors over all measurements for specific product formation rates, 6HA concentrations, 6AHA concentrations, and AA concentrations are 6.6%, 5.7%, 4.9%, and 20.0%, respectively.

Fig. S3. Conversion of 10 mM cyclohexane (A) or cycloheptane (B) under optimized conditions. Panels A and B show product concentrations accumulated after different reaction times. A 1:1 strain ratio was applied for the strain combination *P. taiwanensis*_CL/*E. coli*_CL with a total biomass concentration of 4.0 g l^{-1} in 12.5 ml liquid volume in 250 ml screw-capped and closed flasks. Biotransformations were started by adding 10 mM of cycloalkanes (referred to the aqueous phase volume). Intermediates that are not depicted in the graphs accumulated to less than 50 μM. Panel C shows the courses of oxygen concentrations in the gas phase (solid lines) and of aqueous cyclohexane (C6) and cycloheptane (C7) concentrations (dashed lines). Means and error bars refer to two independent experiments. The average experimental errors over all measurements for 6HA concentrations, 6AHA concentrations, AA concentrations, 7-hydroxyheptanoic acid concentrations, 7-aminoheptanoic acid concentrations, pimelic acid concentrations, oxygen concentrations, cyclohexane concentrations, and cycloheptane concentrations are 67.1, 6.2%, 3.8%, 26.9%, 9.9%, 17.6%, 3.3%, 26.2%, and 12.0%, respectively.

Fig. S4. Conversion of 6HA to AA by *P. taiwanensis* VLB120. Growing cells were inoculated in M9* medium at an OD450 of 0.2. After 2 h of growth (OD450 ~ 0.4, time point 0 h), 1 mM (squares) or 5 mM (triangles) 6HA was added and growth (dashed lines) as well as AA formation (solid lines) were recorded. Means and error bars refer to two independent experiments. The average experimental errors over all measurements for the AA concentration and OD450 are 6.7% and 2.7%, respectively. over all measurements for the AA concentration and OD450 are 6.7% and 2.7%, respectively.

Table S1. Strains and plasmids used in this study.

Table S2. Primers used for cloning.

Table S3. Specifications for biotransformation experiments.

